Reductive N–N bond cleavage and coupling of organic azides mediated by chromium(I) and vanadium(I) β-diketiminate†‡§

Kuan-Ming Lin,[a] Po-Yang Wang,[a] Yun-Jen Shieh,[a] Hong-Zhang Chen,[a] Ting-Shen Kuo[b] and Yi-Chou Tsai*[a]

Received (in Montpellier, France) 12th February 2010, Accepted 5th May 2010
DOI: 10.1039/c0nj00114g

Reactions of organic azides RN_3 with two univalent inverted-sandwich complexes (μ-η^6:η^6-$C_6H_5CH_3$)[M(Nacnac)]$_2$ (M = Cr (**1**) and V (**2**); Nacnac = HC(C(Me)N$C_6H_3{}^iPr_2$)$_2$) have been investigated. Where R = *p*-tolyl, reaction with **1** results in reductive N_2 elimination and the formation of a diimido product Cr(NR)$_2$(Nacnac) and a cycloaddition tetrazene product Cr[N(R)NNN(R)](Nacnac), which can be converted to Cr(NR)$_2$(Nacnac) upon thermolysis. However, reaction of **1** with Me_3SiN_3 does not produce a diimido complex, but a monomeric three-coordinate amido product Cr[N(SiMe$_3$)$_2$](Nacnac) and an azide-bridged dinuclear compound [Cr(μ-N_3)(Nacnac)]$_2$. On the other hand, where R = *p*-tolyl, 1-adamantyl, or SiMe$_3$, reaction with the more reducing **2** gives solely a diimido product V(NR)$_2$(Nacnac). The symmetric diimido complex V(NSiMe$_3$)$_2$(Nacnac) (**10**) can be converted to an asymmetric diimido complex V(NSiMe$_3$)(*N*-2,6-$C_6H_3{}^iPr_2$)[Me$_3$SiNC(Me)C(H)C(Me)N(2,6-$C_6H_3{}^iPr_2$)] (**11**) upon heating.

1. Introduction

Multiply bonded transition metal–nitrogen complexes are an important class of species in many aspects. These complexes have been implicated in many applications, such as nitrogen fixation,[1,2] atom and group transfer reactions,[3–17] and catalysis, such as olefin[18,19] and imine metathesis.[20–22] Of these, transition metal imido complexes have risen to prominence among metal–ligand multiply bonded systems because of the diverse range of chemistry in which they participate.[23,24] One standard strategy for the construction of metal imido functionalities is from organic azides.[23,24] Organic azides are reactive molecules, which are frequently used for the preparation of metal imido complexes *via* a 2-electron oxidation of metals. An organic azide coordinates to a metal centre giving an intermediate adduct M–N_3R which subsequently undergoes an inner sphere electron transfer reaction to liberate dinitrogen and produce a metal imido complex.[25]

In order to achieve the preparation of metal imido complexes, the metal atoms should provide vacant sites for organic azides to bind to metal centres. Moreover, the metal complexes are capable of undergoing 2-electron oxidation. In this regard, low-coordinate and low-valent transition metal complexes are the best candidates for the synthesis of metal imido compounds. For example, Warren *et al.* reported that the β-diketiminate supported univalent cobalt[26] and nickel[27] complexes are good synthons for the preparation of mono-imido complexes, where the imido ligands are from respective organic azides. We recently demonstrated characterization of two inverted sandwich type chromium(I) and vanadium(I) complexes, (μ-η^6:η^6-$C_6H_5CH_3$)[M(Nacnac)]$_2$ (M = Cr (**1**) and V (**2**); Nacnac = HC(C(Me)N$C_6H_3{}^iPr_2$)$_2$).[28,29] Preliminary reactivity studies of these two species establish that they behave as two equivalent of multi-electron reductants, M(Nacnac). For example, monomeric diimido and dioxo complexes were produced from the reactions of (μ-η^6:η^6-$C_6H_5CH_3$)[M(Nacnac)]$_2$ and organic azides, azobenzene, and dioxygen *via* reductive cleavage processes. Meanwhile, Theopold *et al.* also described that β-diketiminate supported chromium imido and dioxo complexes are accessible starting from a chromium(I) dinitrogen complex and azobenzene and dioxygen.[30,31] Herein, more thorough studies on reactions of various organic azides and (μ-η^6:η^6-$C_6H_5CH_3$)[M(Nacnac)]$_2$ giving N–N cleavage, coupling, and N–C coupling and cleavage are reported.

2. Experimental

General information

Unless stated otherwise, all operations were performed using standard Schlenk techniques or in a Vacuum Atmospheres dry box under an atmosphere of nitrogen. Diethyl ether (Et_2O) and tetrahydrofuran (THF) were distilled under nitrogen from purple sodium benzophenone ketyl. *n*-Hexane was distilled under nitrogen from CaH_2. Distilled solvents were transferred under vacuum into vacuum-tight glass vessels before being

---

[a] *Department of Chemistry, National Tsing Hua University, 101, Sec 2, Guang Fu Road, Hsinchu 300, Taiwan. E-mail: yictsai@mx.nthu.edu.tw; Fax: +886 3 5711082; Tel: +886 3 5718232*
[b] *Department of Chemistry, National Taiwan Normal University, 88, Sec 4, Ting-Chou Road, Taipei, 116, Taiwan. E-mail: t42002@ntnu.edu.tw; Fax: +886 2 29324239; Tel: +886 2 77346137*

† In memory of Dr Pascal Le Floch.

‡ This article is part of a themed issue on Main Group chemistry.

§ Electronic supplementary information (ESI) available: X-Ray crystallographic data of **5** (CCDC 764154), **6** (CCDC 764812), **7** (CCDC 764811), **8** (CCDC 764155), **9** (CCDC 764151), **10** (CCDC 764152), and **11** (CCDC 764153) including tables and CIF files. EPR spectrum of **4** and crystal structure of **7**. For ESI and crystallographic data in CIF or other electronic format see DOI: 10.1039/c0nj00114g transferred into a dry box. C_6D_6 was purchased from Aldrich and was degassed and dried over 4 Å sieves. The 4 Å sieves and Celite were dried *in vacuo* overnight at a temperature just above 200 °C. Both inverted-sandwich complexes **1** and **2** were prepared following literature method.[26,27] All other compounds were used as received. ^1H and ^{13}C NMR spectra were recorded on Varian Unity INOVA 500 MHz or Bruker DMX 600 MHz spectrometers at room temperature. ^{13}C NMR spectra are proton decoupled. Chemical shifts of ^1H and ^{13}C spectra are reported with respect to internal solvent: 7.16 ppm and 128.00(t) ppm (C_6D_6) and external solvent: 7.16 ppm for ^2H spectra. X-Band EPR spectra were recorded on a Bruker EMX EPR spectrometer (9.77 GHz) running Win EPR software.

Synthesis of Cr(*N*-*p*-Tol)$_2$(Nacnac) (4) and Cr[η^2-(*N*-*p*-Tol-N)$_2$]-(Nacnac) (5)

A sample of 0.500 g (0.4848 mmol) of **1** was dissolved in 14 mL of diethyl ether in a 20 mL of vial. Meanwhile, a sample of 0.2582 g (1.9392 mmol) of *p*-TolN_3 was dissolved in 4 mL of diethyl ether also in a 20 mL of vial. Both resultant solutions were kept at −35 °C for 30 min. Then, to the stirred solution of **1** was added the *p*-TolN_3 solution. The clear solution quickly turned turbid accompanied with rapid effervescence. It was then stirred for a further 15 h, after which the purple solid (**5**) was collected by filtration and washed by 4 mL of diethyl ether twice. The filtrate was stripped to dryness *in vacuo*, and the resultant solid was dissolved in 10 mL of toluene. Upon heating at 100 °C for two days, the toluene solution became brown and a brown solid was obtained after all volatiles were removed *in vacuo*. The brown solid (**4**) was dissolved in THF, and X-ray quality crystals were obtained by cooling the THF solution to −35 °C. The isolated yield was 32.4% (0.1066 g) in two crops. Anal. calcd for $C_{43}H_{55}N_4Cr$ (**4**): C, 75.96; H, 8.15; N, 8.24%; Found: C, 75.81; H, 8.28; N, 8.20%. $\mu_{eff} = 1.76\ \mu_B$ (Evans' method, C_6D_6). On the other hand, the purple solid **5** was dissolved in THF and the resultant solution was kept at −35 °C, from which X-ray quality crystals were obtained. The isolated yield is 54.3% (0.1863 g) in two crops. Anal. calcd for $C_{43}H_{55}N_6Cr$ (5): C, 72.95; H, 7.83; N, 11.87%; Found: C, 73.13; H, 8.13; N, 11.40%. $\mu_{eff} = 3.69\ \mu_B$ (Evans' method, THF-d_8).

Synthesis of V(NR)$_2$(Nacnac) (R = *p*-Tol, 6; 1-Ad, 7; SiMe$_3$, 10)

General procedure: A sample of 0.4269 g (0.2399 mmol) of **2** was dissolved in 6 mL of diethyl ether in a 20 mL of vial. Meanwhile, a sample of 0.1105 g (0.9591 mmol) of Me_3SiN_3 was dissolved in 4 mL of diethyl ether also in a 20 mL of vial. Both resultant solutions were kept at −35 °C for 30 min. Then, to the stirred solution of **2** was added the Me_3SiN_3 solution. The clear violet solution was stirred at room temperature, during which the solution quickly turned into dark orange accompanied with rapid effervescence. The solution was then stirred for further 4 h, after which all volatiles were removed *in vacuo*, and the resultant orange solid was extracted into 10 mL of n-hexane and the solution was filtered through a bed of Celite. The filtrate was concentrated and kept at −35 °C, from which X-ray quality crystals of **10** were obtained. The isolated yield is 91.0% (0.2808 g) in two crops. ^1H NMR (C_6D_6, 400 MHz, 300 K): δ 7.10 (m, 6 H, 2,6-^{i}Pr$_2$C$_6$*H*$_3$), 5.40 (s, 1 H, *H*C(C(Me)NC$_6$H$_3$^{i}Pr$_2$)$_2$), 3.35 (septet, 4 H, C*H*Me$_2$), 1.63 (s, 6 H, HC(C(*Me*)NC$_6$H$_3$^{i}Pr$_2$)$_2$), 1.43 (d, 12 H, CH*Me*$_2$), 1.18 (d, 12 H, CH*Me*$_2$), 0.19 (s, 18 H, Si*Me*$_3$). $^{13}C\{^1H\}$ NMR (C_6D_6, 100.7 MHz, 300 K): δ 169.67 (*C*=N), 145.39 (*ipso*-C of 2,6-^{i}Pr$_2$C$_6$H$_3$), 142.00 (*ortho*-C of 2,6-^{i}Pr$_2$C$_6$H$_3$), 127.09 (*para*-C of 2,6-^{i}Pr$_2$C$_6$H$_3$), 124.26 (*meta*-C of 2,6-^{i}Pr$_2$C$_6$H$_3$), 102.39 (H*C*(C(Me)NC$_6$H$_3$^{i}Pr$_2$)$_2$), 27.79 (*C*HMe$_2$), 25.58 (CH*Me*$_2$), 24.26 (CH*Me*$_2$), 23.87 (CH*Me*$_2$), 2.40 (Si*Me*$_3$). Anal. Calcd. for $C_{35}H_{59}N_4Si_2V$: C, 65.38; H, 9.25; N, 8.71%. Found: C, 65.20; H, 9.23; N, 8.73%.

Intense yellow X-ray quality crystals of **6** were obtained by slow vaporization of a diethyl ether solution at room temperature. The yield is 34.6% in one crop. ^1H NMR (C_6D_6, 400 MHz, 300 K): δ 7.15 (t, 2 H, *para*-2,6-^{i}Pr$_2$C$_6$*H*$_3$), 7.09 (d, 4 H, *meta*-2,6-^{i}Pr$_2$C$_6$*H*$_3$), 6.83 (d, 4 H, *meta*-4-MeC$_6$H$_4$), 6.74 (d, 4 H, *ortho*-4-MeC$_6$H$_4$), 5.56 (s, 1 H, *H*C(C(Me)NC$_6$H$_3$^{i}Pr$_2$)$_2$), 3.56 (septet, 4 H, C*H*Me$_2$), 2.02 (s, 6 H, HC(C(*Me*)NC$_6$H$_3$^{i}Pr$_2$)$_2$), 1.78 (s, 6 H, 4-*Me*C$_6$H$_4$), 1.24 (d, 12 H, CH*Me*$_2$), 1.17 (d, 12 H, CH*Me*$_2$). $^{13}C\{^1H\}$ NMR (C_6D_6, 100.7 MHz, 300 K): δ 168.50, 162.41, 144.29, 142.50, 131.95, 128.74, 127.07, 124.10, 122.83, 101.01, 28.41, 25.35, 24.33, 24.02, 21.00. ^{51}V NMR: δ −172.28. Anal. calcd. for $C_{43}H_{55}N_4V$: C, 76.08; H, 8.17; N, 8.25%. Found: C, 75.81; H, 8.25; N, 8.39%.

Orange X-ray quality crystals of **7** were obtained by slow vaporization of a diethyl ether solution at room temperature. The yield is 36.2% in one crop. ^1H NMR (C_6D_6, 400 MHz, 300 K): δ 7.15 (m, 6 H, 2,6-^{i}Pr$_2$C$_6$*H*$_3$), 5.49 (s, 1 H, *H*C(C(Me)NC$_6$H$_3$^{i}Pr$_2$)$_2$), 3.58 (septet, 4 H, C*H*Me$_2$), 1.99 (m, 6 H, 1-adamentyl), 1.95 (m, 12 H, 1-adamantyl), 1.69 (s, 6 H, 4-*Me*C$_6$H$_4$), 1.59 (m, 6 H, 1-adamantyl), 1.51 (m, 6 H, 1-adamantyl), 1.48 (d, 12 H, CH*Me*$_2$), 1.22 (d, 12 H, CH*Me*$_2$). $^{13}C\{^1H\}$ NMR (C_6D_6, 100.7 MHz, 300 K): δ 169.20, 147.31, 142.10, 128.51, 126.43, 124.15, 102.52, 71.98, 65.86, 46.48, 36.93, 30.45, 27.62, 25.86, 24.32. ^{51}V NMR: δ −389.73. Anal. calcd. for $C_{49}H_{71}N_4V$: C, 76.73; H, 9.33; N, 7.30%. Found: C, 76.25; H, 9.41; N, 7.35%.

Synthesis of Cr[N(SiMe$_3$)$_2$](Nacnac) (8) and [Cr(μ-N$_3$)(Nacnac)]$_2$ (9)

A sample of 0.5000 g (0.4848 mmol) of **1** was dissolved in 8 mL of diethyl ether in a 20 mL of vial. Meanwhile, a sample of 0.3351 g (2.9090 mmol) of Me_3SiN_3 was dissolved in 2 mL of diethyl ether also in a 20 mL of vial. Both resultant solutions were kept at −35 °C for 30 min. At which point, to the stirred solution of **1** was added the Me_3SiN_3 solution. The clear solution was allowed to stirred at room temperature. The solution was then stirred for further 12 h. At which point, all volatiles were removed *in vacuo*. The resultant solid was added 10 mL of n-hexane, and the suspension was stirred for 1 h. The green solid (**9**) was collected by filtration. The dark yellow filtrate (**8**) was stripped down to dryness under vacuum. Solid **8** was dissolved in 5 mL of $(Me_3Si)_2O$, and the solution was kept at −35 °C for 2 days to afford dark yellow X-ray quality crystals. The yield is 48.0% (0.1467 g) in one crop. $\mu_{eff} = 4.73\ \mu_B$. Anal. calcd for $C_{35}H_{59}N_3Si_2Cr$ (**8**): C, 66.72; H, 9.44; N, 6.67%; Found: C, 66.62; H, 9.39; N, 6.48%.

Green solid **9** was dissolved in 3 mL of THF, and the solution was kept at −35 °C for 3 days to afford green X-ray quality crystals. The yield is 32.7% (0.0406 g) in one crop. μ_{eff} = 6.22 μ_B. Anal. calcd for $C_{58}H_{82}N_{10}Cr_2$ (**9**): C, 68.07; H, 8.08; N, 13.69%; Found: C, 67.87; H, 8.16; N, 13.42%.

Synthesis of V(NTMS)(*N*-Dipp)[N(TMS)C(CH$_3$)CHC(CH$_3$)N-(Dipp)] (Dipp = 2,6-^{i}Pr$_2$C$_6$H$_3$) (11)

A sample of 0.3850 g (0.5988 mmol) of orange **10** was dissolved 8 mL of toluene in a 100 mL of Schlenk flask and heated at 70 °C for 8 h. During which, the orange solution became yellow green over the course of the reaction. After the solution was allowed to cool to room temperature, all volatile materials were removed under vacuum, the residue was extracted into 10 mL of n-hexane, and the solution was filtered through a bed of Celite. The volume of the filtrate was reduced to one half, and then was kept at −35 °C for 1 days to afford yellow green X-ray quality crystals. The yield is 69% (0.2657 g) in one crop. ^{1}H NMR (C$_6$D$_6$, 400 MHz, 300 K): δ 7.14 (d, 2 H, *meta*-2,6-^{i}Pr$_2$C$_6$*H*$_3$), 7.10 (t, 1 H, *para*-2,6-^{i}Pr$_2$C$_6$*H*$_3$), 7.02 (d, 2 H, *meta*-2,6-^{i}Pr$_2$C$_6$*H*$_3$), 6.94 (t, 1 H, *para*-2,6-^{i}Pr$_2$C$_6$*H*$_3$), 5.53 (s, 1 H, Me$_3$SiNC(Me)(*H*)CC(Me)NC$_6$H$_3$^{i}Pr$_2$), 3.86 (septet, 2 H, C*H*Me$_2$), 3.20 (septet, 1 H, C*H*Me$_2$), 2.83 (septet, 1 H, C*H*Me$_2$), 2.11 (s, 3 H, Me$_3$SiNC(*Me*)(H)CC(Me)NC$_6$H$_3$^{i}Pr$_2$), 1.59 (s, 3 H, Me$_3$SiNC(Me)(H)CC(*Me*)NC$_6$H$_3$^{i}Pr$_2$), 1.37 (d, 6 H, CH*Me*$_2$), 1.35 (d, 3 H, CH*Me*$_2$), 1.29 (d, 3 H, CH*Me*$_2$), 1.19 (d, 6 H, CH*Me*$_2$), 1.07 (d, 3 H, CH*Me*$_2$), 1.07 (d, 3 H, CH*Me*$_2$), 0.33 (s, 9 H, Si*Me*$_3$), 0.10 (s, 9 H, Si*Me*$_3$). ^{13}C{^{1}H} NMR (C$_6$D$_6$, 100.7 MHz, 300 K): δ 172.58 (*C*=N), 171.03 (*C*=N), 145.85 (*ipso*-C of 2,6-^{i}Pr$_2$C$_6$H$_3$), 141.09 (*ipso*-C of 2,6-^{i}Pr$_2$C$_6$H$_3$), 140.44 (*ortho*-C of 2,6-^{i}Pr$_2$C$_6$H$_3$), 140.44 (*ortho*-C of 2,6-^{i}Pr$_2$C$_6$H$_3$), 139.37 (*ortho*-C of 2,6-^{i}Pr$_2$C$_6$H$_3$), 139.30 (*ortho*-C of 2,6-^{i}Pr$_2$C$_6$H$_3$), 127.19 (*para*-C of 2,6-^{i}Pr$_2$C$_6$H$_3$), 124.45 (*meta*-2,6-C$_6$H$_3$^{i}Pr$_2$), 123.85 (*meta*-2,6-^{i}Pr$_2$C$_6$H$_3$), 122.91 (*para*-2,6-C$_6$H$_3$^{i}Pr$_2$), 122.33 (*meta*-2,6-C$_6$H$_3$^{i}Pr$_2$),122.91 (*para*-2,6-C$_6$H$_3$^{i}Pr$_2$), 122.33 (*meta*-2,6-C$_6$H$_3$^{i}Pr$_2$), 108.94 (Me$_3$SiNC(Me)(H)*C*C(Me)NC$_6$H$_3$^{i}Pr$_2$), 28.39 (*C*HMe$_2$), 27.98 (*C*HMe$_2$), 27.78 (*C*HMe$_2$), 27.70 (Me$_3$SiNC(Me)(H)CC(*Me*)-NC$_6$H$_3$^{i}Pr$_2$), 25.72 (CH*Me*$_2$), 24.52 (CH*Me*$_2$), 24.45 (CH*Me*$_2$), 24.20 (CH*Me*$_2$), 24.17 (CH*Me*$_2$), 23.68 (CH*Me*$_2$), 22.86 (Me$_3$SiNC(*Me*)(H)CC(Me)NC$_6$H$_3$^{i}Pr$_2$), 3.20 (Si*Me*3), 2.69 (Si*Me*$_3$). Anal. calcd. for C$_{35}$H$_{59}$N$_4$Si$_2$V: C, 65.38; H, 9.25; N, 8.71%. Found: C, 65.27; H, 9.24; N, 8.46%.

Crystallographic structure determinations

The chosen crystals were mounted on a glass fiber. Data collection were carried out on a NONIUS Kappa CCD diffractometer[32] with Mo radiation (λ = 0.71073 Å) at 200(2) K. Cell parameters were retrieved and refined using *DENZO-SMN* software[33] on all observed reflections. Data reduction was performed with the *DENZO-SMN* software.[33] An empirical absorption was based on the symmetry-equivalent reflections and applied the data using the *SORTAV* program.[34] Using *SHELXTL* program[35] on PC computer made the structure analysis. The structure was solved using the *SHELXS-97* program[36] and refined using *SHELXL-97* program[37] by full-matrix least squares on F^2 values. All of non-hydrogen atoms are refined anisotropically. Hydrogen atoms attached to the carbons were fixed at calculated positions and refined using a riding mode.

3. Results and discussion

3.1 Reactions of 1 and 2 with organic azides

We have demonstrated that the reaction of **1** with sterically encumbered mesityl azide (N$_3$Mes) quickly gave rise to the formation of a tetrahedral chromium(V) diimido complex, Cr(NMes)$_2$(Nacnac) (**3**).[28] Complex **3** features one linear and one bent imido functionalities. This methodology to metal diimido complexes provides a good opportunity to systematically study the geometry of the imido ligands and their reactivity by tuning their electronic and steric factors. A series of organic azides with different substituents are then examined. When 4 equivalents of *p*-tolyl azide (*p*-TolN$_3$) are mixed with **1**, two products are actually isolated. One is the diimido complex Cr(*N*-*p*-Tol)$_2$(Nacnac) (**4**) in 32% yield, and the other is a tetraazametallacyclopentene complex Cr[η^2-(*N*-*p*-Tol-N)$_2$]-(Nacnac) (**5**) in 54% yield as shown in Scheme 1. Though complex **4** is not structurally characterized by single crystal X-ray crystallography, its structure can be confirmed by EPR spectroscopy (see Fig. S1, ESI§) in comparison with that of complex **3**. The room temperature EPR spectrum of **4** in THF displays an isotropic signal at g_{iso} = 1.98036. The spectrum is attributable to coupling of the unpaired electron to two magnetically equivalent ^{14}N nuclei of the Nacnac ligand and two nonequivalent ^{14}N nuclei of the two imido ligands. Successful simulation of the observed spectrum is achieved by specifying four hyperfine couplings: $A_{iso}[^{53}Cr, 9.54\%]$ = 5.0 G, $A_{iso}[^{14}N, 99.63\%]$ = 3.3 G (two from the Nacnac ligands), $A_{iso}[^{14}N, 99.63\%]$ = 1.9 G, and $A_{iso}[^{14}N, 99.63\%]$ = 1.3 G. The sterically encumbered Dipp substituents of the β-diketiminate apparently prohibit equilibration of the two imido groups in solution on the EPR time scale. Accordingly, we speculate that its solid state structure features one bent and one linear imido functionalities. It is noteworthy that having two different imido ligands is common for diimido complexes in the solid state, however, the two imido groups almost invariably equilibrate in solution, based on NMR spectroscopy.[38–40]

Fortunately, the reddish purple tetrazene complex **5** is less soluble in hydrocarbon solvents than **4**, so **5** can be easily separated from **4**. X-Ray quality of crystals were obtained from THF and cooled to −35 °C. An X-ray diffraction study is performed on a single crystal of **5** and an ORTEP view of the structure is provided in Fig. 1. The crystal and data collection parameters are summarized in Table 1. The structure of the tetrazole **5** features CrN$_4$ and CrC$_3$N$_2$ rings that are fused at chromium. The metal has distorted tetrahedral geometry and the Cr–N bonds (1.986(3) Å) to the β-diketiminate nitrogens N(1) and N(2) are significantly longer than the average distance of 1.926(4) Å to the tetrazole nitrogens. The chromium tetrazole ring is essentially planar and the quaternary carbons on both the *p*-tolyl groups also lie in this plane. In contrast, the chromium β-diketiminate six-membered ring C$_3$N$_2$Cr is folded along the N(1)···N(2) axis such that Cr lies *ca.* 0.54 Å out of the averaged N$_2$C$_3$ plane. Consequently, these two rings are not perpendicular to each other with one nitrogen N(3) of the

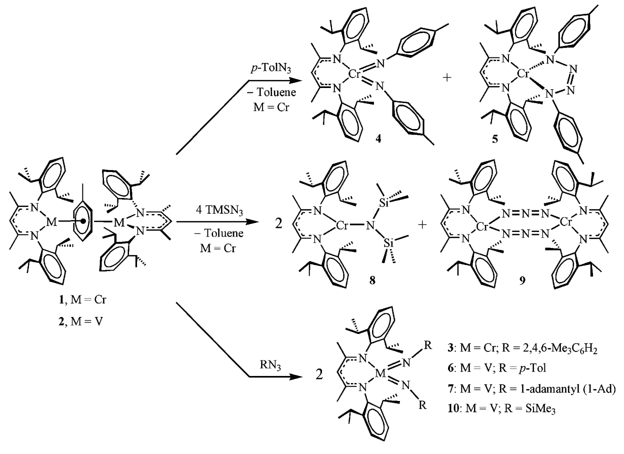

Scheme 1

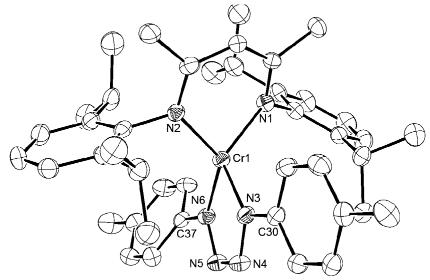

Fig. 1 The molecular structure of **5**, with thermal ellipsoids set at 35% probability and all hydrogen atoms omitted for clarity. Selected bond lengths (Å) and angles (°): Cr(1)–N(1), 1.992(3); Cr(1)–N(2), 1.980(4); Cr(1)–N(3), 1.908(4); Cr(1)–N(6), 1.944(4); N(3)–N(4), 1.376(4); N(4)–N(5), 1.266(6); N(5)–N(6), 1.378(5); N(2)–Cr(1)–N(1), 90.20(17); N(3)–Cr(1)–N(6), 76.42(18); N(2)–Cr(1)–N(6), 130.76(18); N(1)–Cr(1)–N(6), 128.58(17); N(2)–Cr(1)–N(3), 112.07(17); N(3)–Cr(1)–N(1), 120.60(18).

p-tolyl groups being tilted toward the six-membered ring illustrated by two angles C(30)–N(3)–Cr(1), 115.30° and C(37)–N(6)–Cr(1), 168.29°. The N–N bond distances are shortest between the unsubstituted nitrogens, 1.266(6) Å, and somewhat longer between the others, 1.376(6) and 1.378(5) Å. These N–N bond lengths are slightly shorter than those in osmium and zirconium tetrazole complexes (Cymene)Os-[N(^{t}Bu)N═NNPh][41] and Cp*$_2$Zr[N(^{t}Bu)N═NN^{t}Bu],[42] but comparable with those in gallium and germanium tetrazole (Nacnac)Ga[N(TMS)N═NNTMS] (TMS═SiMe$_3$)[43] and Me$_2$Si(^{t}BuN)$_2$Ge[N(^{t}Bu)N═NN(^{t}Bu)].[44] The room temperature solution magnetic moment of 3.99 μ_B of **5** measured by Evans' method indicate it has three unpaired electrons, which is consistent with the oxidation state of Cr center being III. It has been suggested that metallacyclotetraazapentadiene and metallacyclotetraazapentene may contribute to the overall structure of the tetrazole complexes.[45] However, the magnetic moment of **5**, and metric parameters Cr–N(tetrazole) bond lengths of 1.908(4) (Cr(1)–N(3)) and 1.944(4) Å (Cr(1)–Cr(6)) and the double bond N(4)–N(5) distance of 1.266(6) Å, which are comparable with those in tetrazene complexes,[45] support the tetrazole CrN$_4$ ring a metallacyclotetraazapentene instead of a metallacyclotetraazapentadiene.

It is interesting to note that when this reaction is carried out at −10 °C, the isolated yield of **5** is improved to 84%. In contrast, heating **5** in toluene at 100 °C results in the formation of **4** and N$_2$ extrusion. Collectively, it is therefore mechanistically clear as to the reaction of **1** with organic azides. As portrayed in Scheme 2, the first step (1) involves the coordination of an organic azide to give the "diazenylimido" intermediate Cr(η^1-N$_3$R)(Nacnac), which immediately loses N$_2$ to produce a monoimido intermediate Cr(NR)(Nacnac). Addition of another equivalent of organic azide leads to a mechanistic dichotomy. In step 3, the second equivalent of organic azide coordinates to the metal centre also in an η^1 fashion and affords the diazenylimide/imide intermediate Cr(NR)(N$_3$R)(Nacnac), where the diazenylimido ligand subsequently undergoes N$_2$ elimination to engender the formation of diimido complex. It is noteworthy that, although a diazenylimido complex is unusual, four such compounds have been documented and they all feature bent diazenylimido ligands.[46–49] On the other hand, in step 4, the incoming organic azide and the imdio ligand undergo 1,3-dipolar [3 + 2] cycloaddition addition to generate the tetrazole complex.[41–45] Alternatively, the diimido complex can be isolated from heating the cycloaddition tetrazole product *via* N$_2$ extrusion. As a result, the formation of complex **3** is believed directly from the diazenylimido intermediate Cr(NMes)(N$_3$Mes)(Nacnac), which does not undergo the [3 + 2] cycloaddition reaction primarily due to the sterically encumbered mesityl substituent.

Though the proposed monoimido complexes are not observed upon treatment of **1** or **2** with organic azides, the characterization of the cycloaddition tetrazene product **5** proves the formation of the monoimido complexes over the course of the reactions.

Bergman *et al.* have thoroughly studied the [3 + 2] cycloaddition of monomeric Os- and Zr-imido complexes with organic azides featuring various substituents.[41,42] However, it is interesting to note that in Bergman's systems, mononuclear diimido complexes have never been generated from the cycloaddition tetrazole products. For example, the tetrazole complexes (Cymene)Os[N(^{t}Bu)N═NN(R)] are thermally robust,[41] but Cp$_2$Zr[N(^{t}Bu)N═NN(R)] undergo retro [3 + 2] cycloaddition reaction to give monoimido complexes.[42] Moreover, related observations in the main group, the reaction of Ga(Nacnac) with TMSN$_3$ and Me$_2$Si(^{t}BuN)$_2$Ge with *p*-TolN$_3$ also give the tetrazole complexes (Nacnac)Ga[N(TMS)N═NN(TMS)][43] and Me$_2$Si(^{t}BuN)$_2$Ge[N(*p*-Tol)N═NN(*p*-Tol)],[44] respectively. It is probable that these two reactions proceed *via* a common imido intermediate (Nacnac)GaNTMS[43] and Me$_2$Si(^{t}BuN)$_2$GeN-*p*-Tol.[44] The failure to isolate the vanadium tetrazole analogues implies that they immediately undergo N$_2$ elimination to give diimido complexes upon formation. These observations also suggest that V(Nacnac) fragment is much more reducing than Cr(Nacnac).

Interestingly, treatment of the inverted sandwich vanadium analogue **2** with *p*-TolN$_3$ at room temperature gives solely the diimido complex V(*N*-*p*-Tol)$_2$(Nacnac) (**6**) accompanied with the evolution of N$_2$ as shown in Scheme 1; no other vanadium containing products from this reaction at −10 °C are detected by NMR spectroscopy. Crystals of suitable for X-ray diffraction analysis were obtained by crystallization from THF and cooled to −35 °C. The crystallographic data are included in

Table 1 Crystal and data collection parameters

Compound	**5**	**6**	**7**	**8**	**9**	**10**	**11**
Empirical formula	$C_{47}H_{63}CrN_6O$	$C_{43}H_{55}N_4V$	$C_{49}H_{71}N_4V$	$C_{35}H_{59}CrN_3Si_2$	$C_{66}H_{98}Cr_2N_{10}O_2$	$C_{35}H_{59}N_4Si_2V$	$C_{35}H_{59}N_4Si_2V$
Fw	780.03	678.85	767.04	630.03	1167.54	642.98	642.98
Space group	$P\bar{1}$	$Pna2_1$	$P2_1/c$	$P2_1/n$	$P\bar{1}$	$P2_1/c$	$P2_1/n$
a/Å	10.8881(5)	19.4976(7)	19.7038(4)	9.1132(9)	12.5550(2)	18.3009(6)	12.2715(3)
b/Å	12.8734(5)	11.2990(4)	10.9155(3)	20.144(2)	15.3520(2)	10.2668(3)	19.3946(5)
c/Å	16.1682(8)	18.3271(6)	23.6118(6)	20.551(2)	20.1740(4)	20.8551(7)	16.4428(5
α (°)	105.496(2)	90	90	90	75.3030(10)	90	90
β (°)	90.870(2)	90	104.1980(10)	90.350(2)	74.1560(10)	96.0850(10)	100.0740(10)
γ (°)	91.470(2)	90	90	90	67.1920(10)	90	90
V/Å^3	2182.58(17)	4037.5(2)	4923.2(2)	3772.7(7)	3399.93(10)	3896.4(2	3853.07(18)
Z	2	4	4	4	2	4	4
T/K	200(2)	200(2)	200(2)	200(2)	200(2)	200(2)	200(2)
λ/Å	0.71073	0.71073	0.71073	0.71073	0.71073	0.71073	0.71073
d_c/g cm^{-3}	1.187	1.117	1.035	1.082	1.140	1.096	1.108
μ/mm^{-1}	0.303	0.278	0.234	0.392	0.367	0.343	0.346
R_1,[a] wR_2[b] ($I > 2\sigma(I)$)	0.0881, 0.2276	0.0586, 0.1513	0.0986, 0.2530	0.0557, 0.1527	0.0925, 0.2523	0.0762, 0.1822	0.0789, 0.1762

[a] $R_1 = \sum\|F_o| - |F_c\|/\sum|F_o|$. [b] $wR_2 = \{\sum[w(F_o^2 - F_c^2)^2]/\sum[w(F_o^2)]\}^{1/2}$. $w = 1/[(\sigma^2(F_o^2) + (aP)^2 + bP)]$, where $P = [\max(F_o^2 \text{ or } 0) + 2(F_c^2)]/3$.

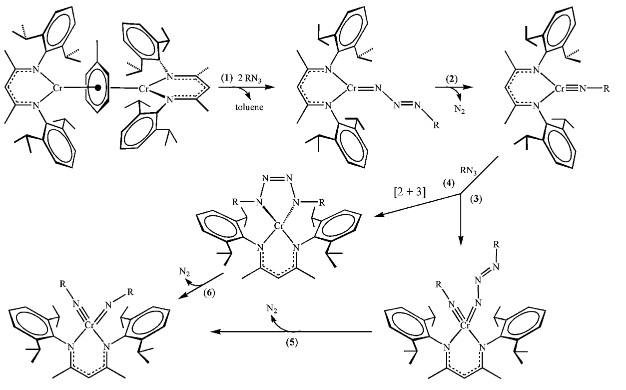

Scheme 2

Table 1, and the molecular structure is shown in Fig. 2. The V–N(imido ligands) bond lengths are 1.677(3) and 1.680(3) Å, respectively. In contrast to chromium diimido complexes **3** and **4** featuring one bent and one linear imido ligands, compound **6** possesses two bent imido ligands with C(37)–N(4)–V(1), 153.7(3)° and C(30)–N(3)–V(1), 157.3(3)°. The vanadium *β*-diketiminate six-membered ring C_3N_2V adopts a puckered conformation with vanadium centre residing 0.66 Å out of the averaged C_3N_2 plane. Complex **6** is fluxional in solution even at low temperature as analyzed by ^1H NMR spectroscopy.

Moreover, when a bulkier organic azide 1-adamantyl azide (1-AdN$_3$) is employed to react with **2**, effervescence is quickly observed and only the diimido complex, V(*N*-1-Ad)$_2$(Nacnac) (**7**) is isolated. The crystal structure of **7** is provided in Fig. S2 (ESI§). Two imido functionalities are essentially linear, C(40)–N(4)–V(1), 170.6(4)° and C(30)–N(3)–V(1), 164.6(4)°, which can be ascribed to the more electron-donating 1-adamantyl substituents. The vanadium centre resides 0.98 Å out of the averaged C_3N_2 plane.

3.2 Reactions of 1 and 2 with trimethylsilyl azide

In contrast with the formation of the diimido complexes **3**, **4**, **6**, and **7** and the tetrazole complex **5** from reactions of

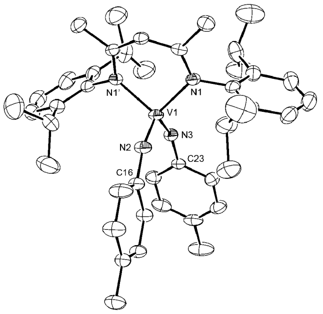

Fig. 2 The molecular structure of **6**, with thermal ellipsoids set at 35% probability and all hydrogen atoms omitted for clarity. Selected bond lengths (Å) and angles (°): V(1)–N(1), 1.986(2); V(1)–N(2), 1.682(4); V(1)–N(3), 1.682(4); V(1)–N(1′), 1.986(3); N(1′)–V(1)–N(1), 97.59(14); N(3)–V(1)–N(1′), 113.24(10); N(2)–V(1)–N(1′), 110.59(11); N(1)–V(1)–N(3), 113.24(10); N(3)–V(1)–N(2), 110.93(18); C(16)–N(2)–V(1), 157.1(3); C(23)–N(3)–V(1), 153.4(3).

(μ-η^6:η^6-$C_6H_5CH_3$)[M(Nacnac)]$_2$ with alkyl- or arylazides, mixing trimethylsilylazide TMSN$_3$ with **1** yields a dark yellow monomeric chromous amide Cr[N(SiMe$_3$)$_2$](Nacnac) (**8**) in 48% yield and a green azide-bridged dinuclear complex [Cr(μ-N$_3$)(Nacnac)]$_2$ (**9**) in 32.7% yield as illustrated in Scheme 1.

Crystals of the amido complex **8** suitable for X-ray diffraction analysis were obtained by crystallization from (Me$_3$Si)$_2$O and cooled to −35 °C. The data collection parameters are included in Table 1 and the structure is shown in Fig. 3. X-Ray structure of **8** shows an unusual three-coordinate Cr(II) center, which adopts a Y-shaped trigonal planar geometry.[50] The chromium *β*-diketiminate ring is also folded along N(1)···N(2) and therefore displays a slightly puckered conformation with the Cr atom residing 0.43 Å out of the averaged C_3N_2 plane. The Cr centre is under effective steric protection by the hexamethyldisilyl amido and *β*-diketiminato ligands, which are arranged in a nearly orthogonal orientation with a N(2)–Cr(1)–N(3)–Si(2) torsion angle of 87.5°. The Cr–N(amido) bond length, 1.963(3) Å, significantly shorter than those of Cr–N(nacnac), 2.001(3) and 2.022(2) Å, suggests a π-bonding interaction between Cr and the amido N atom,

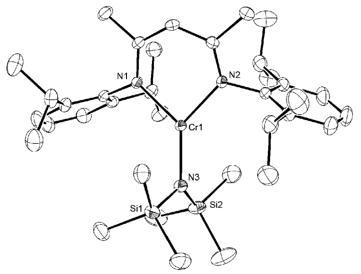

Fig. 3 The molecular structure of **8**, with thermal ellipsoids set at 35% probability and all hydrogen atoms omitted for clarity. Selected bond lengths (Å) and angles (°): Cr(1)–N(3), 1.963(3); Cr(1)–N(2), 2.001(3); Cr(1)–N(1), 2.022(2); N(2)–Cr(1)–N(1), 90.86(10); Si(2)–N(3)–Si(1), 124.61(17); Si(1)–N(3)–Cr(1), 112.61(14); Si(2)–N(3)–Cr(1), 121.68(16).

which dominates the Y-shaped geometry at Cr.[50] All three Cr–N bond lengths are comparable with those of the only example of a three-coordiante amido chromous complex $Cr(NMe_2)(HC(C(^tBu)NC_6H_3{}^iPr_2)_2)$.[50]

As for complex **9**, crystals suitable for X-ray diffraction analysis were obtained by crystallization from THF and cooled to −35 °C. Compound **9** crystallized in the triclinic space group $P\bar{1}$ with two independent molecules in an asymmetric unit: Each lies about an inversion centre. An ORTEP view of one of these two independent molecules is provided in Fig. 4. X-Ray analysis confirms its dimeric structure, and actually shows **9(THF)$_2$** with a weakly bound THF molecule (Cr(1)···O(1) = 2.414(3) Å) at the apical position. The geometry at chromium is square pyramidal with the chromium atom lying 0.40 Å out of the basal plane. Two chromium atom centres are connected together by two coplanar linear azido ligands in an end-on fashion giving rise to a chair confroamtion. All Cr–N bond lengths, 2.058(4)–2.096(4) Å, lie within the range observed for C–N bonds in the literature.[51] Within the N_3 moiety, the N–N distances are similar to those observed in azide-bridged dinuclear complexes.[52] It is noteworthy that the dihedral angle between the plane defined for the six azide N atoms and the N(3)–Cr(1)–N(5′) plane is only 17.9°, suggesting an antiferromagnetic exchange between two Cr centers. The solution magnetic moment of 6.22 μ_B (by Evans' method) of **9** is consistent with this structure-magnetic property correlation.[52]

In analogy to the aforementioned reactions, the first step of reaction of **1** with $TMSN_3$ involves the coordination of one equivalent of $TNSN_3$ to Cr(Nacnac) to give the diazenylimido intermediate $Cr(\eta^1\text{-}N_3TMS)$(Nacnac), which either subsequently eliminates one equivalent of N_2 and gives the monoimido intermediate Cr(NTMS)(Nacnac), or undergoes TMS radical extrusion to produce the chromous azide intermediate $Cr(\eta^1\text{-}N_3)$(Nacnac), which subsequently dimerizes to give complex **9**. On the other hand, reduction of the monoimido intermediate Cr(NTMS)(Nacnac) by a TMS radical leads to the formation of complex **8**.

It is interesting to note that the highly reducing vanadium inverted-sandwich complex **2** exhibits a different reaction with $TMSN_3$ from its chromium analogue. An orange diimido complex $V(NTMS)_2$(Nacnac) (**10**) is isolated in high yield (91%) upon treatment of violet **2** with 4 equivalents of $TMSN_3$ accompanied with N_2 evolution. As assayed by ^1H NMR spectroscopy, complex **10** shows one imido ligand and a symmetric Nacnac, suggesting fluxonal property of **10** in solution on NMR time scale. Crystals of complex **10** suitable for X-ray diffraction analysis were obtained by crystallization from *n*-hexane at −35 °C. The data collection parameters are included in Table 1 and the structure is shown in Fig. 5. The geometry at the vanadium centre displays a distorted tetrahedron. The six-membered ring C_3N_2V displays a highly puckered conformation with the V atom residing 0.93 Å out of the averaged C_3N_2 plane. Unlike the diimido complexes **6** and **7**, which display two bent (**6**) and two linear (**7**) imido functionalities, complex **10** displays one distinctive bent (Si(2)–N(4)–V(1), 143.8(2)°) and one linear (Si(1)–N(3)–V(1), 165.3(2)°) imido ligand, which is rather reminiscent of the structures of compounds **3** and **4**. Presumably, electron donating nature of the imido group dominates the conformation. The alkyl imide, N-1-Ad, of **7** is more electron donating than the corresponding imido ligands of **6** and **10**, so compound **7** features two linear imido ligands. The longer pair of V–N distances to the imide nitrogen atoms 1.706(4) Å, among all V–N(imido) bonds herein, averagely 1.680 Å, is consistent with the observed bent imido nature. Collectively, in contrast with the reaction of complex **1** with organic azides discussed herein, V(Nacnac) is so reducing that only diimido vanadium(V) *β*-diketiminate complexes are isolated regardless of the nature of the organic azides.

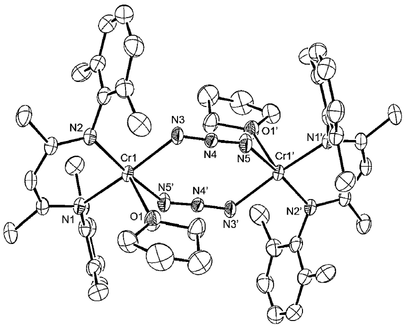

Fig. 4 Two independent molecules of **9** crystallize in an asymmetric unit, and each lies about an inversion centre in the crystal. Displacement ellipsoids of one molecular structure with an intrinsic inversion centre are shown at 35% probability and all hydrogen atoms and CH_3 groups of $2,6\text{-}^iPr_2C_6H_3$ omitted for clarity. Selected bond lengths (Å) and angles (°): Cr(1)–N(1), 2.058(4); Cr(1)–N(2), 2.066(4); Cr(1)–N(5′), 2.096(4); Cr(1)–N(3), 2.096(4); N(3)–N(4), 1.162(5); N(4)–N(5), 1.168(5); Cr(1)···O(1), 2.414(3); N(2)–Cr(1)–N(1), 91.12(15); N(1)–Cr(1)–N(5′), 90.20(16); N(2)–Cr(1)–N(5′), 171.09(18); N(1)–Cr(1)–N(3), 172.01(17); N(2)–Cr(1)–N(3), 90.16(16); N(5A)–Cr(1)–N(3), 87.34(17).

Since one of the imido groups of **10** exhibits bent conformation, the sp^2 hybridized N atom was thus expected to be a good nucleophile, and this is indeed the case. Heating a toluene solution of **10** at 70 °C for 8 h leads to a color change from orange to yellow-green. As assayed by ^1H NMR spectroscopy, compound **10** was completely consumed and transformed into product **11** with two distinctive ligand environments, two different trimethylsilyl substituents, and two different 2,6-diisopropylphenyl groups. Crystals of complex **11** suitable

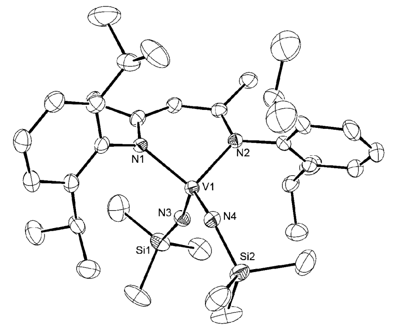

Fig. 5 The molecular structure of **10**, with thermal ellipsoids set at 35% probability and all hydrogen atoms omitted for clarity. Selected bond lengths (Å) and angles (°): V(1)–N(1), 1.986(3); V(1)–N(2), 1.991(3); V(1)–N(3), 1.682(4); V(1)–N(4), 1.706(4); N(2)–V(1)–N(1), 94.79(14); N(4)–V(1)–N(2), 110.73(16); N(3)–V(1)–N(2), 107.67(16); N(1)–V(1)–N(4), 118.61(16); N(3)–V(1)–N(1), 109.14(16); N(3)–V(1)–N(4), 113.89(18); Si(1)–N(3)–V(1), 165.3(3); Si(2)–N(4)–V(1), 143.8(2).

for X-ray diffraction analysis were obtained by crystallization from n-hexane cooled to −35 °C. The data collection parameters are presented in Table 1 and the structure is shown in Fig. 6. The molecular structure of **11** unambiguously indicates the formulation of **11** as V(NTMS)(*N*-Dipp)[N(TMS)C(CH$_3$)CHC(CH$_3$)N(Dipp)] (Dipp = 2,6-^{i}Pr$_2$C$_6$H$_3$) featuring two different imido ligands and a new unsymmetric *β*-diketiminato ligand, which is consistent with the ^{1}H NMR spectrum. The structure of **11** shows a tetrahedral environment of the metal centre. The six-membered ring C$_3$N$_2$V heavily distorts from planar conformation with the vanadium centre lying 1.05 Å away from the averaged C$_3$N$_2$ plane. Notably, this is the longest distance among all complexes herein, and this arrangement is a consequence of reduction of the steric repulsion between both imido functionalities and the unsymmetric Nacnac ligand. It is noteworthy that such an unsymmetric *β*-diketiminato ligand with a silyl group attached to one nitrogen atom is unprecedented, because it is synthetically difficult to achieve.^{53} Not surprisingly, complex **11** also displays one bent imido –NDipp, V(1)–N(3)–C(21), 151.7(3)°, and one linear imido –NTMS, V(1)–N(4)–Si(2), 160.5(2)°.

In order to understand the mechanism as to the intriguing transformation from compound **10** to **11**, the kinetics of this reaction are investigated. The kinetics of this conversion process were studied by monitoring the disappearance of starting species **10** in C$_6$D$_6$ relative to the internal ferrocene standard in the temperature range 343–363 K. In all instances, the reaction follows simple first-order for over two to three half-lives as shown in Fig. 7a. The corresponding Eyring plot is shown in Fig. 7b, from which the activation parameters $\Delta H^\ddagger$ = 112.65 ± 1.06 kJ mol^{-1} and $\Delta S^\ddagger$ = −5.35 ± 2.99 J mol^{-1} K are obtained. As a result, transformation from **10** to **11** unambiguously proceeds *via* an intramolecular ligand rearrangement process. Shown in Scheme 3 is the possible transition state for this transformation. Interestingly, this reaction does not occur to the other diimido complexes reported herein. Therefore, presumably, the sp^2 hybridized nitrogen atom of the bent imido ligand behaves as a nucleophile, which attacks C-2 of the *β*-diketiminate and subsequently undergoes a functional group exchange.

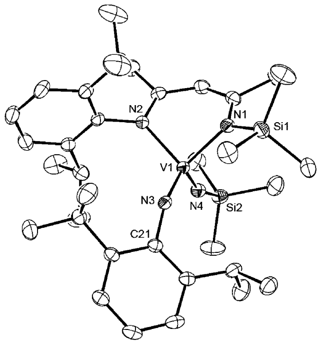

Fig. 6 The molecular structure of **11**, with thermal ellipsoids set at 35% probability and all hydrogen atoms omitted for clarity. Selected bond lengths (Å) and angles (°): V(1)–N(1), 1.979(3); V(1)–N(2), 1.979(3); V(1)–N(3), 1.700(3); V(1)–N(4), 1.680(4); N(2)–V(1)–N(1), 92.90(14); N(4)–V(1)–N(2), 108.09(17); N(3)–V(1)–N(2), 113.98(15); N(1)–V(1)–N(4), 109.01(16); N(3)–V(1)–N(1), 116.15(15); N(3)–V(1)–N(4), 114.53(17); C(21)–N(3)–V(1), 151.7(3); Si(2)–N(4)–V(1), 160.5(2).

Conclusions

In conclusion, we have demonstrated a protocol to prepare chromium and vanadium *β*-diketiminate diimido complexes. We illustrate the ability of both inverted-sandwich complexes **1** and **2** to engage in the reductive N$_2$ elimination of organic azides to form ultimate diimido complexes M(NR)$_2$(Nacnac) (M = Cr, V; R = *p*-Tol, 1-adamantyl, SiMe$_3$), in particular, for the vanadium derivative **2**. It is interesting to note that in contrast with the consistency in diimido products **6**, **7**, and **10** from reaction between **2** and regular organic azides, the reaction between **1** and organic azides displays complicated results. Though the chromium *β*-diketiminate diimido complexes **3** and **4** are obtained, judicious choice of organic azides has allowed for the isolation and X-ray structural characterization of a representative tetrazole complex **5**, by which such tetrazole compound is believed to be an important intermediate of reactions of **1** and **2** with organic azides. Moreover, the reaction of **1** and TMSN$_3$ does not produce the corresponding diimido species, but an unusual mononuclear three-coordinate chromous amide **8** and an azide-bridged dinuclear chromous complex **9**. These results provide valuable insights in to the mechanism of double reductive N$_2$ extrusion of organic azides to form diimido complexes by univalent early transition metals.

It is interesting to note that the synthesized diimido complexes display three combinations in the geometry of two imido ligands, namely, two bent (**6**), two linear (**7**), and one bent and one linear (**10**, **11**). The geometry of the metal imido

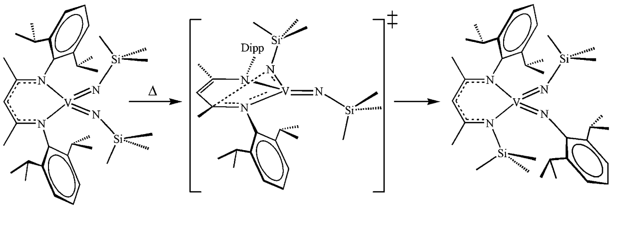

Scheme 3

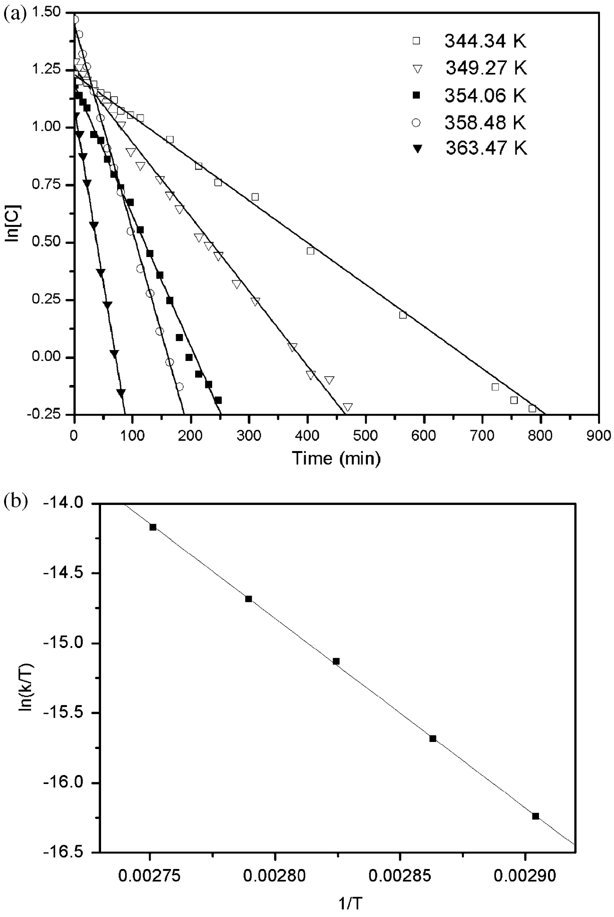

Fig. 7 Kinetic plots (a) and Eyring plot (b) of the reaction **10** → **11**.

linkage M≡N–R (bent *vs.* linear) seems dependent on the electron releasing ability of –NR. The more electron donating R such as 1-adamantyl group exhibits the more linear M≡N–R functionality. The distinctive bent imido group of **10** displays nucleophilic nature, and it attacks the ancillary β-diketiminate upon heating to lead to an intramolecular ligand rearrangement. Future work will accordingly focus on reactivity study of these diimido complexes and, particularly, their capability of effecting interesting organic transformations.

Acknowledgements

We are indebted to the National Science Council, Taiwan for support under Grant NSC 96-2113-M-007-019-MY3.

References

1 *Catalytic Ammonia Synthesis*, ed. J. R. Jennings, Plenum, New York, 1991.
2 C. E. Laplaza and C. C. Cummins, *Science*, 1995, **268**, 861.
3 L. K. Woo, *Chem. Rev.*, 1993, **93**, 1125.
4 L. K. Woo and J. G. Goll, *J. Am. Chem. Soc.*, 1989, **111**, 3755.
5 L. K. Woo, J. G. Goll, D. J. Czapla and J. A. Hays, *J. Am. Chem. Soc.*, 1991, **113**, 8478.
6 L. K. Woo, *Inorg. Chem.*, 1990, **29**, 3915.
7 C. J. Chang, D. L. Low and H. B. Gray, *Inorg. Chem.*, 1997, **36**, 270.
8 F. L. Neely and L. A. Bottomley, *Inorg. Chem.*, 1997, **36**, 5432.
9 F. L. Neely and L. A. Bottomley, *Inorg. Chim. Acta*, 1992, **192**, 147.
10 L. A. Bottomley and F. L. Neely, *J. Am. Chem. Soc.*, 1989, **111**, 5955.
11 L. A. Bottomley and F. L. Neely, *Inorg. Chem.*, 1997, **36**, 5435.
12 C. E. Laplaza, A. R. Johnson and C. C. Cummins, *J. Am. Chem. Soc.*, 1996, **118**, 709.
13 C. R. Clough, J. B. Greco, J. S. Figueroa, P. L. Diaconesco, W. M. Davis and C. C. Cummins, *J. Am. Chem. Soc.*, 2004, **126**, 7742.
14 J. S. Figueroa, N. A. Piro, C. R. Clough and C. C. Cummins, *J. Am. Chem. Soc.*, 2006, **128**, 940.
15 J. J. Curley, E. L. Sceats and C. C. Cummins, *J. Am. Chem. Soc.*, 2006, **128**, 14036.
16 J. J. Silvia and C. C. Cummins, *J. Am. Chem. Soc.*, 2009, **131**, 446.
17 J. J. Silvia and C. C. Cummins, *J. Am. Chem. Soc.*, 2010, **132**, 2169.
18 R. R. Schrock, *Chem. Rev.*, 2009, **109**, 3211.
19 R. R. Schrock and A. H. Hoveyda, *Angew. Chem., Int. Ed.*, 2003, **42**, 4592.
20 G. K. Cantrell and T. Y. Meyer, *Chem. Commun.*, 1997, 1551.
21 G. K. Cantrell and T. Y. Meyer, *Organometallics*, 1997, **16**, 5381.
22 G. K. Cantrell and T. Y. Meyer, *J. Am. Chem. Soc.*, 1998, **120**, 8035.
23 D. E. Wigley, *Prog. Inorg. Chem.*, 1994, **42**, 239.
24 R. A. Eikey and M. M. Abu-Omar, *Coord. Chem. Rev.*, 2003, **243**, 83.
25 S. Cenini, E. Gallo, A. Caselli, F. Ragaini, S. Fantauzzi and C. Piangiolino, *Coord. Chem. Rev.*, 2006, **250**, 1234.
26 X. Dai, P. Kapoor and T. H. Warren, *J. Am. Chem. Soc.*, 2004, **126**, 4798.
27 E. Kogut, H. L. Wiencko, L. Zhang, D. E. Cordeau and T. H. Warren, *J. Am. Chem. Soc.*, 2005, **127**, 11248.
28 Y.-C. Tsai, P.-Y. Wang, S.-A. Chen and J.-M. Chen, *J. Am. Chem. Soc.*, 2007, **129**, 8066.
29 Y.-C. Tsai, P.-Y. Wang, K.-M. Lin, S.-A. Chen and J.-M. Chen, *Chem. Commun.*, 2008, 205.
30 W. H. Monillas, G. P. A. Yap, L. A. MacAdams and K. H. Theopold, *J. Am. Chem. Soc.*, 2007, **129**, 8090.
31 W. H. Monillas, G. P. A. Yap and K. H. Theopold, *Angew. Chem., Int. Ed.*, 2007, **46**, 6692.
32 *COLLECT*, Nonius BV, Delft, The Netherlands, 2003.
33 Z. Otwinowski and W. Minor, *Methods Enzymol.*, 1997, **276**, 307.
34 SORTAV: R. H. Blessing, *Acta Crystallogr., Sect. A: Found. Crystallogr.*, 1995, **51**, 33.
35 *SHELXTL: Structure analysis program, version 6.10*, Bruker-axs, Madison, WI, 2000.
36 SHELXS-97: G. M. Sheldrick, Phase annealing in *SHELX*-90, *Acta Crystallogr., Sect. A: Found. Crystallogr.*, 1990, **46**, 467.
37 G. M. Sheldrick, *SHELXL-97, Program for refinement of crystal structures*, University of Göttingen, Germany, 1997.
38 D. C. Bradley, S. R. Hodge, J. D. Runnacles, M. Hugees, J. Mason and R. L. Richrds, *J. Chem. Soc., Dalton Trans.*, 1992, 1663.
39 P. Barrie, T. A. Coffey, G. D. Forster and G. Hogarth, *J. Chem. Soc., Dalton Trans.*, 1999, 4519.
40 J. B. Strong, G. P. A. Yap, R. Ostrander, L. M. Liable-Sands, A. L. Rheingold, R. Thouvenot, P. Gouzerh and E. A. Maata, *J. Am. Chem. Soc.*, 2000, **122**, 639.
41 R. L. Michelman, R. G. Bergman and R. A. Andersen, *Organometallics*, 1993, **12**, 2741.
42 K. E. Meyer, P. J. Walsh and R. G. Bergman, *J. Am. Chem. Soc.*, 1995, **117**, 974.
43 N. J. Hardman and P. P. Power, *Chem. Commun.*, 2001, 1184.
44 B. Klein and W. P. Neumann, *J. Organomet. Chem.*, 1994, **465**, 119.
45 W. C. Trogler, *Acc. Chem. Res.*, 1990, **23**, 426 and references therein.
46 G. Proulx and R. G. Bergman, *J. Am. Chem. Soc.*, 1995, **117**, 6382.
47 G. Proulx and R. G. Bergman, *Organometallics*, 1996, **15**, 684.

48 M. G. Fickes, W. M. Davis and C. C. Cummins, *J. Am. Chem. Soc.*, 1995, **117**, 6384.

49 G. Guillemot, E. Solari, C. Floriani and C. Rizzoli, *Organometallics*, 2001, **20**, 607.

50 H. Fan, D. Adhikari, A. A. Saleh, R. L. Clark, F. J. Zuno-Cruz, G. Sanchez Cabrera, J. C. Huffman, M. Pink, D. J. Mindiola and M.-H. Baik, *J. Am. Chem. Soc.*, 2008, **130**, 17351.

51 V. C. Gibson, C. Newton, C. Redshaw, G. A. Solan, A. J. P. White and D. J. Williams, *Eur. J. Inorg. Chem.*, 2001, 1895.

52 J. Ribas, A. Escuer, M. Monfort, R. Vicente, R. Cortés, L. Lezama and T. Rojo, *Coord. Chem. Rev.*, 1999, **193–195**, 1027.

53 L. Bourget-Merle, M. F. Lappert and J. R. Severn, *Chem. Rev.*, 2002, **102**, 3031.